

Studies of the ammonia decomposition over a mixture of α – Fe(N) and γ' – Fe₄N

Karolina Kielbasa*, Walerian Arabczyk

West Pomeranian University of Technology, Szczecin, Institute of Chemical and Environment Engineering, Pułaskiego 10, 70-322 Szczecin, Poland

* Corresponding author: kkielbasa@zut.edu.pl

An industrial pre-reduced iron catalyst for ammonia synthesis was nitrided in a differential reactor equipped with the systems that made it possible to conduct both the thermogravimetric measurements and hydrogen concentration analyser in the reacting gas mixture. The nitriding process, particularly the catalytic ammonia decomposition reaction, was investigated under an atmosphere of ammonia-hydrogen mixtures, under the atmospheric pressure, at 475°C. The nitriding potentials were changed gradually in the range from $19 \cdot 10^{-3}$ to $73 \cdot 10^{-3}$ Pa^{-0.5} in the reactor for an intermediate area where two phases exist simultaneously: Fe(N) and γ' -Fe₄N. In the area wherein $P > 73 \cdot 10^{-3}$ Pa^{-0.5}, approximately stoichiometric composition of γ' – Fe₄N phase exists and saturating of that phase by nitrogen started. The rate of the catalytic ammonia decomposition was calculated on the basis of grain volume distribution as a function of conversion degree for that catalyst. It was found that over γ' – Fe₄N phase in the stationary states the rate of catalytic ammonia decomposition depends linearly on the logarithm of the nitriding potential. The rate was decreasing along with increase in the nitriding potential. For the intermediate area, the rate of ammonia decomposition is a sum of the rates of reactions which occur on the surfaces of both Fe(N) and γ' – Fe₄N.

Keywords: catalytic ammonia decomposition; kinetics; iron catalyst.

INTRODUCTION

In review papers, studies on ammonia decomposition kinetic over various catalysts have been shown^{1, 2}. Ammonia decomposition is an important reaction in science and technology thanks to its involvement in lots of industrial applications e. g. removing of pollutants from exhaust gases³ and ammonia-containing waste gases⁴⁻⁸, fuel – cells technology^{1, 2, 9-16}, producing of controlled atmospheres for heat treatment in metallurgical industry¹⁷ and biomass gasification as well¹⁸.

The catalytic ammonia decomposition has been studied extensively for the last couple of decades. Works elaborated before 1990s were mostly connected with the explorations of kinetics of the ammonia synthesis¹⁹. However, in last forty years the investigations were focused on studies of the nitriding process²⁰⁻²³ and NH₃ abatement^{6, 24}. Studies of the ammonia decomposition are directly relevant to a better understanding of the mechanism of ammonia synthesis thus that reaction was studied under different conditions: thermal²⁵⁻²⁷, catalytic¹¹, photo-chemical²⁸, and in plasma²⁹. Several catalysts have been proposed: ruthenium^{30, 31}, iridium³², iron^{19, 23, 33-38}, nickel³⁹, platinum^{32, 39} and rhodium as well⁴⁰. Fused catalysts which indicate high activity in ammonia decomposition reaction have been also investigated^{41, 42}.

In previous works ammonia decomposition, as a parallel reaction to nitriding reaction in the iron catalyst nitriding process, was studied^{43, 44}. It was found that during the process in question, ammonia diffuses from the gas phase to the surface of the catalyst. Then ammonia adsorbs on the surface of iron crystallites and then ammonia dissociation to atomic hydrogen and nitrogen occurs (the dissociative adsorption process). Atoms of hydrogen form particles which then desorb. Nitrogen atoms may combine to form particles which then desorb or react with iron to create solid solution of nitrogen in iron or iron nitrides.

The rate of the catalytic ammonia decomposition reaction over iron depends on many factors such as, for instance, composition and purity of the gas phase, a specific surface area and composition of catalyst on which reaction proceeds. The influence of water vapour in the gas phase⁴⁵ and sulfur adsorbed on solid surface^{46, 47} on the rate of ammonia decomposition process was analyzed. The catalytic ammonia decomposition reaction proceeds with different rates depending on the solid phase present in the nitriding process⁴⁸.

Ammonia decomposition kinetic studies are available in the literature and most of those descriptions are focused on low ammonia concentrations and/or low temperature. Based on the published data on catalytic ammonia synthesis and decomposition the following conclusions can be drawn^{1, 2, 49}:

– at low ammonia partial pressures and low temperatures the rate of catalytic ammonia decomposition can be described by equation^{19, 50}:

$$r = \frac{kKP_{NH_3}}{1 + KP_{NH_3}} \quad (1)$$

where k is reaction rate constant and K is adsorption constant.

In that case, the order of the reaction with respect to ammonia equals zero and at temperature higher than 500°C the order of the reaction increases to unity.

– at high hydrogen pressure and low temperatures the Temkin – Pyzhev law can be applied^{51, 52}:

$$r = kP; \quad P = \frac{P_{NH_3}}{P_{H_2}^{3/2}} \quad (2)$$

where k is reaction rate constant and P is nitriding potential.

The information in literature does not take into account changes of state of catalyst which occur during the process. In our previous work⁵³ it was found that nitriding

degree of iron catalyst (ratio of moles of nitrogen to moles of iron in sample) is a function of the nitriding potential (the gas phase composition influences on the nitriding degree of solid samples) and temperature as well⁵⁴. It was observed that three areas of various composition of catalyst exist in the range of nitriding potential from 2.9×10^{-5} to $0.06 \text{ Pa}^{-0.5}$, at 475°C :

1st – $P < 19 \cdot 10^{-3} \text{ Pa}^{-0.5}$ the observed nitriding degree is relatively low and equals less than $0.015 \text{ mol}_\text{N}/\text{mol}_\text{Fe}$, what corresponds to the nitrogen dissolving and ammonia adsorption on the surface of iron. The nitriding reaction did not occur.

2nd – P from $19 \cdot 10^{-3} \text{ Pa}^{-0.5}$ to $73 \cdot 10^{-3} \text{ Pa}^{-0.5}$ the nitriding reaction started up. Two phases exist simultaneously in the catalyst: Fe(N) and $\gamma' - \text{Fe}_4\text{N}$.

3rd – $P > 73 \cdot 10^{-3} \text{ Pa}^{-0.5}$, approximately stoichiometric composition of $\gamma' - \text{Fe}_4\text{N}$ phase was observed and saturating of the nitride by nitrogen started.

It was concluded that the rate dependences for ammonia decomposition available in the literature do not reflect our data. Thus new empirical logarithmic equation was proposed (Fig. 1)⁵³. The rate of the ammonia decomposition reaction over the Fe(N) phase has been described by the expression⁵³:

$$r_{\text{Fe(N)}} = 3.5 \cdot 10^{-5} + 2.4 \cdot 10^{-6} \ln P \quad (3)$$

When the values of the nitriding potential were increasing, the rate of catalytic ammonia decomposition on $\alpha - \text{Fe(N)}$ was increasing as well.

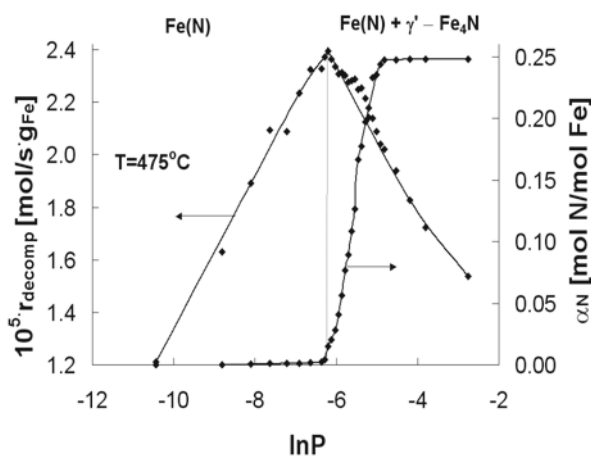


Figure 1. The dependence of the nitriding degree of solid sample and the rate of ammonia decomposition reaction on the logarithm of nitriding potential (ammonia – hydrogen mixtures in the reactor)⁵³

In the range where two phases ($\alpha - \text{Fe(N)}$ and $\gamma' - \text{Fe}_4\text{N}$) exist simultaneously and in the region where γ' is saturated by nitrogen the rate of the ammonia decomposition depends non - linearly on the logarithm of the nitriding potential.

The subject of the present considerations is the analysis of the kinetics of the catalytic ammonia decomposition reaction in the area where two phase exist ($\alpha - \text{Fe(N)}$ and $\gamma' - \text{Fe}_4\text{N}$ nitride) because the kinetics of the ammonia decomposition reaction over that mixture have not been yet successfully described.

EXPERIMENTAL METHODS

The kinetic of the catalytic ammonia decomposition was investigated making use of a tubular differential reactor equipped with a gas phase composition analyser and a system that made it possible to conduct the thermogravimetric measurements. In the platinum basket hanging on a thermobalance arm approximately 1 g of the analysed material (an industrial pre-reduced iron catalyst for ammonia synthesis was studied; apart from metallic iron the catalyst contains promoter's oxides: 3.3% wt. Al_2O_3 , 2.8% wt. CaO , 0.65% wt. K_2O) was placed in a form of a single layer of grains with size in the range of 1.0–1.2 mm. The samples of the gas phase were collected from sampling points which were located in direct neighborhood of catalyst. Flow – rate of the gas reactants was regulated making use of electronic mass flow controllers. Detailed description of the experimental part is available in our previous paper⁵³.

Nitriding process was preceded by a polythermal reduction of a passive layer from the analysed solid samples. The temperature of the reduction was up to 500°C . The reduction process was performed under hydrogen atmosphere ($p_{\text{H}_2} = 1$), under atmospheric pressure.

The nitriding process was performed in the temperature 475°C , under atmospheric pressure. Ammonia – hydrogen mixtures containing various quantity of ammonia (in the range of 0–100%) were let into the reactor.

RESULTS AND DISCUSSION

Catalytic ammonia decomposition over iron catalyst for ammonia synthesis was studied. Apart from metallic nanocrystalline iron the reduced sample contains promoter's oxides. The structural promoters prevent the iron nanocrystallites from sintering thus the material has an average size of iron nanocrystallites of 20 nm and the values of specific surface area is $12 \text{ m}^2 \text{ g}^{-1}$. Nanocrystalline structure of the catalyst is stable in the temperatures lower than the reduction temperature, in that case it is 500°C .

It was found that during nitriding process carried out in 475°C nitriding reaction started up at the minimum nitriding potential $P_0 = 19 \cdot 10^{-3} \text{ Pa}^{-0.5}$. According to adsorption range model^{55–57}, the dissociative adsorption of ammonia on the iron catalyst is a limiting step. Inside nanocrystallites there is no concentrations gradient of nitrogen. Phase transition of crystallites saturated by nitrogen is observed when critical bulk concentration of nitrogen is reached. The minimum nitriding potential necessary to initiate the phase transition depends on nanocrystallites' size. In smaller crystallites the critical concentration of a gaseous reactant is reached earlier than in greater ones. Therefore crystallites undergo the phase transition in the order of the smallest to the greatest. Nanocrystallites structure of Fe(N) underwent the transition from bcc lattice system to fcc. Nitride γ' is obtained as a result of saturation of the fcc lattice system by nitrogen.

After the reduction process (hydrogen left in the reactor.) ammonia – hydrogen mixtures containing various quantities of ammonia were allowed to the reactor. Therefore, different compositions of catalyst were

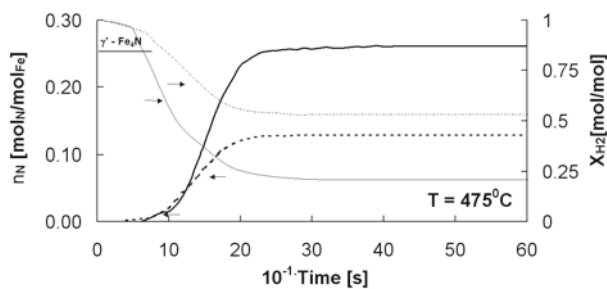


Figure 2. The nitriding degree and hydrogen concentration versus time (100% ammonia at the reactor inlet – solid lines, 53% ammonia at the reactor inlet – dashed lines; T = 475°C, p = 1 atm)

observed. Some exemplary results of those experiments are shown in Fig. 2.

Initially, the gas mixing process occurred simultaneously with two parallel reactions – nitriding and catalytic ammonia decomposition. Consequently, changes of gas phase composition and nitriding degree occur. Concentration of hydrogen was decreasing until the constant value was reached. When a stable mass of the solid sample is observed (the nitriding reaction rate is zero) and only catalytic ammonia decomposition with constant rate occurs on a given nitrated phase, then the stationary state is achieved. In the stationary state, the equilibrium between gas phase and solid sample exists, but catalytic ammonia decomposition reaction is still running.

The rate of the catalytic ammonia decomposition changes along with the changes of the catalyst's composition. Therefore, the commonly known equation describing the rate of ammonia decomposition in 2nd and 3rd area has to be reinterpreted and divided into two separate equations, one for each of the areas. In 1st area, where Fe(N) exists, the rate is described by Eq. 3. In turn, in 3rd area the following logarithmic equation is proposed:

$$r_{\gamma'} = 5.2 \cdot 10^{-6} - 3.1 \cdot 10^{-6} \ln P \quad (4)$$

For mixture of two phases: Fe(N) and $\gamma' - Fe_4N$ (2nd area), it was assumed that measured value of the rate of ammonia decomposition is a sum of rates of reactions which occur on the surfaces of both Fe(N) and $\gamma' - Fe_4N$:

$$r_{Fe(N)+\gamma'} = S_{Fe(N)} r_{Fe(N)} + S_{\gamma'} r_{\gamma'} \quad (5)$$

where $S_{Fe(N)}$ and $S_{\gamma'}$ are the surface fraction of Fe(N) and $\gamma' - Fe_4N$ phases.

To evaluate the surface fraction, the grain volume distribution as a function of conversion degree (α) for that catalyst has to be provided. This crystallites' distribution for the same sample has been elaborated (Fig. 3a)⁵⁸.

It was found that specific surface area determined by Thermal Desorption (single point BET method on PEAK – 4 apparatus) has different values from the specific surface area determined by XRD (X – Ray Diffraction apparatus with copper lamp, X'Pert PRO). Thus to get the measured specific surface area of the catalyst equals 12 m² g⁻¹, the shape coefficient has to be assumed. On that basis and knowing the grain volume distribution as a function of conversion degree, the distribution of crystallites' surface area of studied catalyst was determined (Fig. 3b).

The integral in Fig. 3b is represented as the area of the region bounded by its graph and has the same value as the measured specific surface area. There was assumption

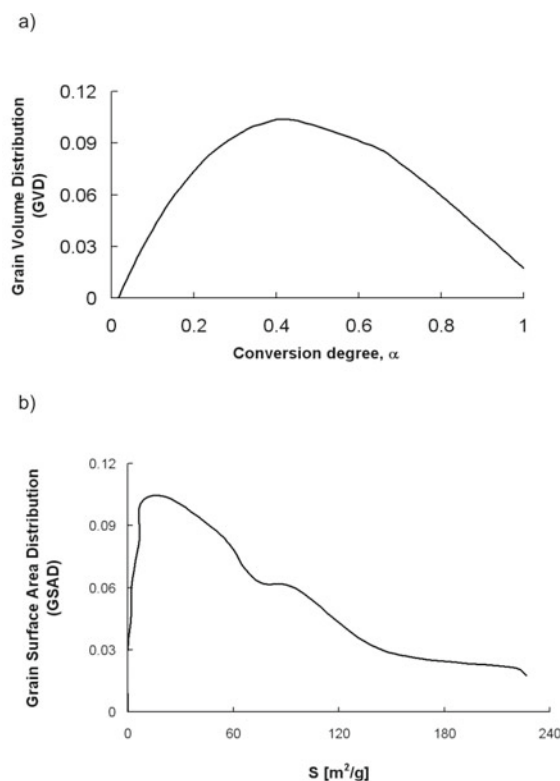


Figure 3. a) Grain volume distribution⁵⁸ b) Grain surface area distribution

that the specific surface area is stable both before and after the nitriding process. Taking under consideration the above issues the surface fractions were determined:

$$S_{Fe(N)} = f(\alpha) \cdot \int_0^{1-\alpha} f(GSAD) d\alpha \quad (6)$$

$$S_{\gamma'} = f(1-\alpha) \cdot \int_{1-\alpha}^{\alpha} f(GSAD) d\alpha \quad (7)$$

When the values of the surface fraction of Fe(N) and $\gamma' - Fe_4N$ phases were known, the rates of ammonia decomposition reaction were calculated making use of the Equations 3–7 and have been shown in Fig. 4 with black points.

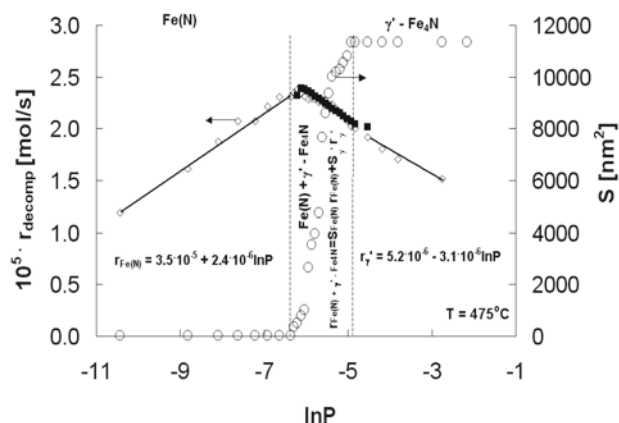


Figure 4. The dependence of the surface of solid sample and the rate of ammonia decomposition reaction on the logarithm of nitriding potential (ammonia – hydrogen mixtures in the reactor)

The calculated values of the rate of catalytic ammonia decomposition match the experimental data well, thus it can be assumed that our considerations are correct.

CONCLUSIONS

According to the results of kinetic analysis of catalytic ammonia decomposition, it was found that over γ -Fe₄N phase in the stationary states the rate of catalytic ammonia decomposition depends on the logarithm of the nitriding potential. The rate was decreasing along with an increase in the nitriding potential. For the intermediate area, where two phases exist simultaneously, the rate of ammonia decomposition is a sum of the rates of reactions which occur on the surfaces of both Fe(N) and γ -Fe₄N.

LITERATURE CITED

1. Yin, S.F., Xu, B.Q., Zhou, X.P. & Au C.T. (2004). A mini-review on ammonia decomposition catalysts for on-site generation of hydrogen for fuel cell applications. *Appl. Catal. A* 277, 1–9. DOI: 10.1016/j.apcata.2004.09.020.
2. Chellappa, A.S., Fisher, C.M. & Thomson, W.J. (2002). Ammonia decomposition kinetics over Ni-Pt/Al₂O₃ for PEM fuel cell applications. *Appl. Catal.* 227, 231–40.
3. Jennings, J.R. (Ed.). (1991). *Catalytic Ammonia Synthesis*. New York, USA: Plenum Press.
4. Currey, J.H. (1991). Ammonia destruction at citizens gas and coke utility. *Iron Steel Eng.* 68 (7), 43–45.
5. Li, Y. & Armor, J.N. (1997). Selective NH₃ oxidation to N₂ in a wet stream. *Appl. Catal. B* 13, 131–137.
6. Mojtahedi, W. & Abbasian, J. (1995). Catalytic decomposition of ammonia in a fuel gas at high temperature and pressure. *Fuel* 74 (11), 1698–1703. DOI: /10.1016/0016-2361(95)00152-U.
7. Svoboda, K.P. & Diemer, P.E. (1990). Catalytic decomposition of ammonia from coke-oven gas. *Iron Steel Eng.* 12, 42–46.
8. Armor, J.N. (1994). *Environmental catalysis*. Washington, USA: ACS.
9. Szmigiel, D., Raróg-Pilecka, E., Kowalczyk, Z., Jodzis, S. & Zieliński, J. (2004). Ammonia decomposition over the ruthenium catalysts deposited on magnesium-aluminum spinel. *Appl. Catal.* 264, 59–63. DOI: 10.1016/j.apcata.2003.12.038.
10. Raróg-Pilecka, Szmigiel, D.E., Kowalczyk, Z., Jodzis, S. & Zieliński, J. (2003). Ammonia decomposition over the carbon-based ruthenium catalyst promoted with barium or cerium. *J. Catal.* 218, 465–469. DOI: 10.1016/S0021-9517(03)00058-7.
11. Ganley, J.C., Thomas, F.S., Seebauer, E.G. & Masel, R.I. (2004). A priori catalytic activity correlations: the difficult case of hydrogen production from ammonia. *Catal Lett.* 96, 117–122. DOI: 10.1023/B:CATL.0000030108.50691.d4.
12. Choudhary, T.V., Sivadinarayana, C. & Goodman, D.W. (2001). Catalytic ammonia decomposition: CO_x-free hydrogen production for fuel cell applications. *Catal. Lett.* 72, 197–201.
13. Choudhary, T.V., Sivadinarayana, C. & Goodman, D.W. (2003). Production of CO_x-free hydrogen for fuel cells via step-wise hydrocarbon reforming and catalytic dehydrogenation of ammonia. *Chem. Eng. J.* 93, 69–80.
14. Deshmukh, S.R., Mhadeshwar, A.B. & Vlachos, D.G. (2004). Microreactor modeling for hydrogen production from ammonia decomposition on ruthenium. *Ind. Eng. Chem. Res.* 43, 2986–2999.
15. Sorensen, R.Z., Nielsen, L.J.E., Jensen, S., Hansen O., Johannessen, T., Quaade, U. & Chrisyensen, C.H. (2005). Catalytic ammonia decomposition: miniaturized production of CO_x-free hydrogen for fuel cells. *Catal. Commun.* 6, 229–232. DOI: 10.1016/j.catcom.2005.01.005.
16. Yin, S.F., Zhang, Q.H., Xu, B.Q., Zhu, W.X., Ng, Ch.F. & Au, C.T. (2004). Investigation on the catalysis of CO_x-free hydrogen generation from ammonia. *J. Catal.* 224, 384–396.
17. Kiyoshi, N., Hiroyuki, F. & Akio, N. (1979). *Highly purity hydrogen*, JP79. 126.689.
18. Wang, W., Padban, N., Andersson, A. & Bjerle, I. (1999). Kinetics of Ammonia Decomposition in Hot Gas Cleaning. *Ind. Eng. Chem. Res.* 38, 4175–4182.
19. Löffler, D.G. & Schmidt, L.D. (1976). Kinetics of NH₃ decomposition on polycrystalline Pt. *J. Catal.* 41, 440–454.
20. Oyama, S.T. (1992). Kinetics of ammonia decomposition on vanadium nitride. *J. Catal.* 133, 358–369.
21. Djega-Mariadassou, G., Shin, C.H. & Bugli, G. (1999). Tamaru's model for ammonia decomposition over titanium oxynitride. *J. Mol. Catal. A: Chem.* 141, 263–267.
22. Wise, R.S. & Markel, E.J. (1994). Catalytic NH₃ decomposition by topotactic molybdenum oxides and nitrides: effect on temperature programmed γ -Mo₂N synthesis. *J. Catal.* 145, 335–343.
23. Arabczyk, W. & Zamlyny, J. (1999). Study of the ammonia decomposition over iron catalysts. *Catal. Lett.* 60, 167–171.
24. Simell, P.A., Hepola, J.O. & Krause, A.O.I. (1997). Effects of gasification gas components on tar and ammonia decomposition over hot gas cleanup catalysts. *Fuel* 76, 1117–1127.
25. Hinshelwood, C.N. & Burk, R.E. (1925). The thermal decomposition of ammonia upon various surfaces. *J. Chem. Soc.* 127, 1105–1117. DOI: 10.1039/CT9252701105.
26. Cooper, D.A. & Ljungstrom, E.B. (1988). Decomposition of NH₃ over Quartz Sand at 840–960°C *Energy Fuels* 2, 716–719.
27. Dirtu, D., Odochian, L., Pui, A. & Humelnicu, I. (2006). Thermal decomposition of ammonia. N₂H₄ – an intermediate reaction product. *Cent. Eur. J. Chem.* 4, 666–673. DOI: 10.2478/s11532-006-0030-4.
28. Bonhoeffer, K.F. & Farkas, L.Z. (1928). The interpretation of diffuse molecular spectra. Experiments on the photochemical decomposition of ammonia. *Physik. Chem.* 134, 337–344.
29. Giquel, A., Saillard, P. & Laidani, N. (1989). Mechanism of catalytic decomposition in an NH₃ low pressure plasma. *Rev. Phys. Appl.* 24, 285–294.
30. Bradford, M.C.J., Fanning, P.E. & Vannice, M.A. (1997). Kinetics of NH₃ decomposition over well dispersed. Ru. *J. Catal.* 172, 479–484.
31. Tsai, W. & Weinberg, W.H. (1987). Steady-state decomposition of ammonia on the Ru(001) surface. *J. Phys. Chem.* 91, 5302–5307.

32. Papapolymerou, G. & Bontontozolou, V. (1997). Decomposition of NH_3 on Pd and Ir comparison with Pt and Rh. *J. Mol. Catal. A* 120, 165–171.
33. Ohtsuka, Y., Xu, C., Kong, D. & Tsubouchi, N. (2001). *Am. Chem. Soc. Div. Fuel Chem. Prepr.* 46, 151.
34. Grunze, M., Bozso, F., Ertl, G. & Weiss, M. (1978). Interaction of ammonia with Fe(111) and Fe(100) surfaces. *Appl. Surf. Sci.* 1, 241–265.
35. Weiss, M., Ertl, G. & Nitschke, F. (1979). Adsorption and decomposition of ammonia on Fe(110). *Appl. Surf. Sci.* 2, 614–635.
36. Ertl, G. & Huber, M. (1980). Mechanism and kinetics of ammonia decomposition on iron. *J. Catal.* 61, 537–539.
37. Kowalczyk, Z., Sentek, J., Jodzis, S., Muhler, M. & Hinrichsen, O. (1997). Effect of potassium on the kinetics of ammonia synthesis and decomposition over fused iron catalyst at atmospheric pressure. *J. Catal.* 169, 407–414.
38. Kowalczyk, Z. (1996). Effect of potassium on the high pressure kinetics of ammonia synthesis over fused iron catalyst. *Catal. Lett.* 37, 173–179.
39. Tsai, W., Vajo, J. & Weinberg, W.H. (1985). Inhibition by Hydrogen of the heterogeneous decomposition of ammonia on platinum. *J. Phys. Chem.* 89, 4926–4932.
40. Vavere, A. & Hansen R.S. (1981). Decomposition of ammonia on rhodium crystals. *J. Catal.* 69, 158–171.
41. Willey, R.J. & Fox, M.F.I.I. (1988). Ammonia decomposition over 430-ss etched metal catalysts *J. Catal.* 112, 590–594.
42. Liang, Ch., Li, W., Wei, Z., Xin, Q. & Li, C. (2000). Catalytic decomposition of ammonia over nitrified $\text{MoNx}/\alpha\text{-Al}_2\text{O}_3$ and $\text{NiMoNy}/\alpha\text{-Al}_2\text{O}_3$ catalyst. *Ind. Eng. Chem. Res.* 39, 3694–3697.
43. Arabczyk, W. & Pelka, R. (2009). Studies of the kinetics of two parallel reactions: ammonia decomposition and nitriding of iron catalyst. *J. Phys. Chem. A.* 113, 411–416.
44. Pelka, R. & Arabczyk, W. (2009). Studies of the kinetics of reaction between iron catalysts and ammonia - nitriding of nanocrystalline iron with parallel catalytic ammonia decomposition. *Top. Catal.* 52, 1506–1516. DOI: 10.1007/s11244-009-9297-y.
45. Arabczyk, W., Zamlynny, J., Moszyński, D. & Kałucki, K. (2005). Ammonia decomposition over iron in the presence of water vapor. *Polish J. Chem.* 79, 1495–1501.
46. Arabczyk, W., Zamlynny, J. & Moszyński, D. (2006). The influence of hydrogen sulphide on the kinetics of ammonia decomposition over a doubly promoted iron catalyst. *Polish J. Chem.* 80, 345–350.
47. Arabczyk, W., Moszyński, D., Narkiewicz, U., Pelka, R. & Podsiadły, M. (2007). Poisoning of iron catalyst by sulfur. *Catal. Today* 124, 43–48. DOI: 10.1016/j.cattod.2007.02.003.
48. Pelka, R., Moszyńska, I. & Arabczyk, W. (2009). Catalytic ammonia decomposition over Fe/Fe₄N. *Catal. Lett.* 128, 72–76.
49. Tamaru, K. (1988). A “new” general mechanism of ammonia synthesis and decomposition on transition metals. *Acc. Chem. Res.* 21, 88–94.
50. Löffler, D.G. & Schmidt, L.D. (1976). Kinetics of NH_3 decomposition on iron at high temperatures. *J. Catal.* 44, 244–258.
51. Temkin, M.I. & Pyzhev, V. (1939). Kinetics of the synthesis of ammonia on promoted iron catalysts *Jour. Phys. Chem.*, 13, 851–867.
52. Temkin, M.I. & Pyzhev, V. (1940). Kinetics of the synthesis of ammonia on promoted iron catalysts. *Acta Physiochem.* 34, 6512.
53. Kiełbasa, K., Pelka, R. & Arabczyk, W. (2010). Studies of the kinetics of ammonia decomposition on promoted nanocrystalline iron using gas phases of different nitriding degree. *J. Phys. Chem. A.* 114, 4531–4534. DOI: 10.1021/jp9099286.
54. Moszyńska, I., Moszyński, D. & Arabczyk, W. (2009). Hysteresis in nitriding and reduction in the nanocrystalline iron-ammonia-hydrogen system. *Przem. Chem.* 88, 526–529.
55. Wróbel, R. & Arabczyk, W. (2006). Solid-gas reaction with adsorption as the rate limiting step. *J. Phys. Chem. A.* 110, 9219–9224.
56. Arabczyk, W. & Wróbel, R. (2003). Study of the kinetics of nitriding of nanocrystalline iron using the TG and XRD methods. *Solid State Phenomena.* 94, 185–188.
57. Arabczyk, W. & Wróbel, R. (2003). Utilization of XRD for the determination of the size distribution of nanocrystalline iron materials. *Solid State Phenomena.* 94, 235–238.
58. Pelka, R., Moszyński, D. & Arabczyk, W. (2010). Letter of PL patent application no. P 393391.